

Technical Communication

Ultimate bearing capacity of a strip footing placed on sand with a rigid basement



Feng Yang, Xiang-Cou Zheng, Lian-Heng Zhao*, Yi-Gao Tan

School of Civil Engineering, Central South University, Changsha, Hunan Province, People's Republic of China

ARTICLE INFO

Article history:

Received 10 December 2015
 Received in revised form 6 April 2016
 Accepted 11 April 2016
 Available online 28 April 2016

Keywords:

Shallow strip footing
 Finite element upper-bound method
 Rigid translatory moving elements
 Ultimate bearing capacity
 Failure mechanism
 Rigid basement

ABSTRACT

The bearing capacity factor (N_γ), correction factor (K_γ), and failure mechanism of a strip footing with a rigid basement were investigated using UBFEM-RTME. The footing–sand interface and the sand–basement interface were assumed perfectly rough. The results are presented in terms of the variations of N_γ and K_γ with the friction angle, ϕ , and dimensionless thickness, h/b , of the sand. When h/b is smaller than dimensionless critical depth H_{cr}/b , N_γ and K_γ increase with decreasing h/b or increasing ϕ and the mesh-like failure mechanism is found to confine within a small domain.

© 2016 Elsevier Ltd. All rights reserved.

1. Introduction

The ultimate bearing capacity of shallow strip footings is a classic issue that plays a considerably vital role in geotechnical and civil engineering. Previous investigations on this problem mainly focused on footings on purely cohesive soil and frictional soil [1–8]. However, strip footings are usually not placed on a semi-infinite solid bed but are more commonly confined either horizontally or vertically. Note that this issue has received considerable attention, especially in the case of horizontal confinement [9–11]. Their investigations demonstrated that horizontal confinement has a significant effect on the bearing capacity of strip footings.

At an engineering site, however, strip footings are often placed on a sand layer with a hard stratum basement such as stiff rock. Even though failures of strip footing may occur at a rock mass [12], these kinds of basement are seen as perfectly rigid in present analysis, and their failures are assumed to be confined and occur only at the sand layer. With the constraints imposed by the rigid basement, the failure mechanisms for strip footings become much more complex and ultimate bearing capacities are difficult to determine. Little information has been reported on this issue. The available reports were presented by Salencon [9] and Mandel and

Salencon [13]. Thus, it is necessary to further determine the ultimate bearing capacities and associated failure mechanisms.

In this study, the ultimate bearing capacity of shallow strip footings placed on purely frictional sand with a rigid basement was investigated using the upper-bound finite element method with rigid translatory moving elements (UBFEM-RTME) that introduced by Yang et al. [14]. The footing–sand interface and the sand–basement were assumed to be perfectly rough. The upper-bound solutions for the bearing capacity factor N_γ and the correction factor K_γ for a series of friction angles (ϕ) and dimensionless thicknesses (h/b) of the sand layer were determined using nonlinear programming, and the associated failure mechanisms were simultaneously obtained. These upper-bound solutions were compared with results available in literature.

2. Problem definitions

The theoretical models for a rough strip footing with a rigid basement placed on a sand layer and the associated major failure surfaces are presented in Fig. 1. The half and whole width of the footing are separately denoted by parameters b and B . The footing–sand interface is assumed perfectly rough, and the thickness of the sand layer is h . The rigid basement surface is assumed horizontal, and its contact with the sand is also assumed perfectly rough. The width of the failure mechanisms on the ground surface is defined by w .

* Corresponding author. Tel.: +86 13755139425.

E-mail address: zhaolianheng@csu.edu.cn (L.-H. Zhao).

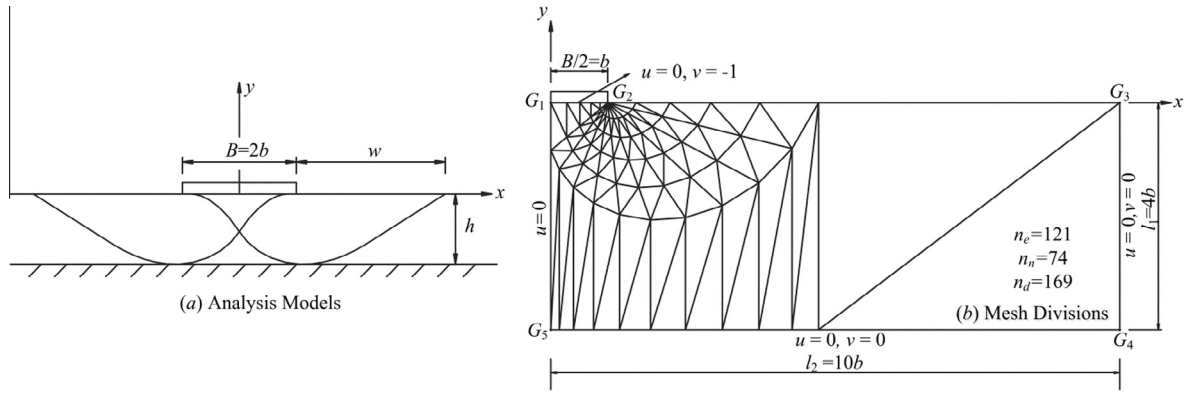


Fig. 1. Models and mesh divisions for the bearing capacity of strip footing with rigid basement.

When the ultimate loading, q_u , is applied on a rigid strip footing without a rigid basement, the footing moves downward vertically, and the scope of its failure mechanism spreads downward to a critical depth, H_{cr} , which depends on the friction angle, ϕ , of the sand. Under the assumption that the sand obeys the associated flow rule, the bearing capacity factor $N'_\gamma(\phi)$ for a strip footing without a rigid basement can be given as:

$$N'_\gamma(\phi) = \frac{2q_u}{\gamma B}, \quad (1)$$

where γ is the unit weight of sand.

If the rigid basement is located at a dimensionless distance of $h/b < H_{cr}/b$, the scope of the failure mechanisms and the ultimate bearing capacity of the footing are moderately affected. Given this effect on the capacity of the strip footing,

$$N_\gamma(\phi) = K_\gamma(h/b, \phi) N'_\gamma(\phi), \quad (2)$$

where $N_\gamma(\phi)$ is the bearing capacity factor for a strip footing with a rigid basement, and $K_\gamma(h/b, \phi)$ is the correction factor that depends on value ϕ and parameter h/b .

To facilitate analysis, only the right half of the problem domain with initial mesh divisions was considered (presented in Fig. 1(b)). A Cartesian coordinate system with its origin located at point G_1 was employed. This domain was artificially discretized into a number of three-node rigid triangular elements. The mesh divisions for the footings with rigid basements are identical to those without rigid basements. For the latter, however, the nodal coordinates above the sand-basement interface were confined by geometric constraints. To obtain a better upper-bound solution and an optimized failure mechanism, the mesh was optimized through a series of amendments in the calculation process. To summarize the mesh optimization results, the domain depth (l_1) and length (l_2) were set equal to $4b$ and $10b$, respectively. The total numbers of elements, nodes, and velocity discontinuities defined by the parameters n_e , n_n , and n_d , respectively, were also included in this figure.

3. Models for N_γ by UBFEM-RTME

Recently, based on the upper-bound kinematical theorem of limit analysis, Yang et al. [14] introduced the UBFEM-RTME. By directly setting the coordinates of the elements' nodes and the velocities of the elements as unknowns to be determined and applying geometric constraints to guarantee the forms of the meshes and elements, the optimal locations for velocity discontinuities were obtained through automatic searches using nonlinear programming.

According to the upper-bound theorem, the present upper-bound solutions are always greater than the theoretical solutions. An upper-bound solution of the bearing load on a rigid strip footing can be obtained by equating the power done by the bearing load to the power done by the soil weight. The ultimate bearing capacity ($q_{u \min}$), using the UBFEM-RTME based on nonlinear programming, is defined as

$$q_{u \min} = \sum_{i=1}^{n_e} P_{e,i}/b, \quad (3)$$

where $P_{e,i}$ is the power done by gravity for element $i = -A_i \cdot \gamma \cdot v_i$ and n_e is the total number of elements. A_i is the area of the i th element, v_i is the vertical velocity of the i th element along the upward direction.

The constraints are written as

$$\begin{cases} -\zeta'_i - \zeta''_i \leq 0; \zeta'_i - \zeta''_i \leq 0 (i = 1, \dots, n_d) & (a) \\ -A_i \leq 0 (i = 1, \dots, n_e) & (b) \\ u_i = 0, v_i = -1; 0 \leq x_j \leq b, y_j = 0 (i = 1, \dots, n_{v1}; j = 1, \dots, n_{g1}) & (c) \\ u_i = 0; x_j = 0, -4b \leq y_j \leq 0 (i = 1, \dots, n_{v2}; j = 1, \dots, n_{g2}) & (d) \\ u_i = 0, v_i = 0; 0 \leq x_j \leq 10b, y_j = -4b (i = 1, \dots, n_{v3}; j = 1, \dots, n_{g3}) & (e) \\ u_i = 0, v_i = 0; x_j = 10b, -4b \leq y_j \leq 0 (i = 1, \dots, n_{v4}; j = 1, \dots, n_{g4}) & (f) \\ b \leq x_j \leq 10b, y_j = 0 (j = 1, \dots, n_{g5}) & (g) \\ 0 \leq x_j \leq 10b; -h \leq y_j \leq 0 (j = 0, \dots, n_{g6}) & (h) \end{cases} \quad (4)$$

Eq. (4a) presents the constraints of the velocity discontinuities, where ζ'_i and ζ''_i are auxiliary parameters that used to explain the associated flow rule along velocity discontinuities, and n_d is the total number of velocity discontinuities. Eq. (4b) presents the geometric constraints of the elements; Eq. (4c)–(4g) define the constraints along boundaries G_1G_2 , G_1G_5 , G_4G_5 , G_3G_4 , and G_2G_3 , respectively, where x_j and y_j are nodal coordinates at the geometric boundaries, and n_{v1} and n_{g1} define the total number elements and nodes at the velocity and geometric boundaries, respectively. Eq. (4h) presents the geometric constraints for nodal coordinates above the sand-basement interface. Other variables are precisely the same as those used in Yang et al. [14]. After obtaining the magnitude of $q_{u \min}$, N_γ is then calculated using Eq. (1).

4. Results and discussions

4.1. Comparisons of N'_γ for strip footings without rigid basements

For strip footings without rigid basements, the N'_γ values for different values of ϕ obtained by the UBFEM-RTME are compared in Table 1 with previously reported results using different

Download English Version:

<https://daneshyari.com/en/article/254525>

Download Persian Version:

<https://daneshyari.com/article/254525>

[Daneshyari.com](https://daneshyari.com)